

A Synthetic Zipper Peptide Motif Orchestrated via Co-operative Interplay of Hydrogen Bonding, Aromatic Stacking, and Backbone Chirality

Roshna V. Nair,[†] Sanjeev Kheria,[†] Suresh Rayavarapu,[†] Amol S. Kotmale,[§] Bharatam Jagadeesh,^{||} Rajesh G. Gonnade,[‡] Vedavati G. Puranik,[‡] Pattuparambil R. Rajamohanan,^{*,§} and Gangadhar J. Sanjayan^{*,†}

[†]Division of Organic Chemistry, [‡]Center for Materials Characterization, [§]Central NMR Facility, National Chemical Laboratory, Dr. Homi Bhabha Road, Pune 411 008, India

^{||}Center for NMR and Structural Chemistry, Indian Institute of Chemical Technology, Hyderabad 500 007, India

Supporting Information

ABSTRACT: Here, we report on a new class of synthetic zipper peptide which assumes its three-dimensional zipper-like structure via a co-operative interplay of hydrogen bonding, aromatic stacking, and backbone chirality. Structural studies carried out in both solid- and solution-state confirmed the zipper-like structural architecture assumed by the synthetic peptide which makes use of unusually remote inter-residual hydrogen-bonding and aromatic stacking interactions to attain its shape. The effect of chirality modulation and the extent of non-covalent forces in the structure stabilization have also been comprehensively explored via single-crystal X-ray diffraction and solution-state NMR studies. The results highlight the utility of noncovalent forces in engineering complex synthetic molecules with intriguing structural architectures.

Engineering complex synthetic molecules which can adopt a preferred three-dimensional (3D) architecture and function has long attracted the attention of chemists.¹ Use of noncovalent interactions in enforcing structural rigidity to such artificial frameworks would not only expand the scope of their structural intricacy² but would also help increase our understanding of biomolecular folding and function.^{3–5}

The functional property of biopolymers is dictated by their specific 3D architecture, orchestrated by the co-operative interplay of a collection of noncovalent forces.⁶ Among the various noncovalent interactions which play key roles in the structural assembly and function of biopolymers, directional hydrogen-bonding (H-bonding)⁷ and the sequence-dependent aromatic stacking interactions,⁸ assume importance. An archetypical example is Nature's sophisticated DNA zipper assembly, wherein the H-bonds self-complementarily intermingle to direct a duplex formation and the aromatic–aromatic interactions driving the template organization.⁹ Double-helical assemblies emulating such architectures have permitted their applications to extend from the field of developing aptamers¹⁰ to molecular shuttles.¹¹ Besides these, solvophobic interactions¹² and van der Waals forces also occupy their domain in distinct cases, resulting in the structure and function of

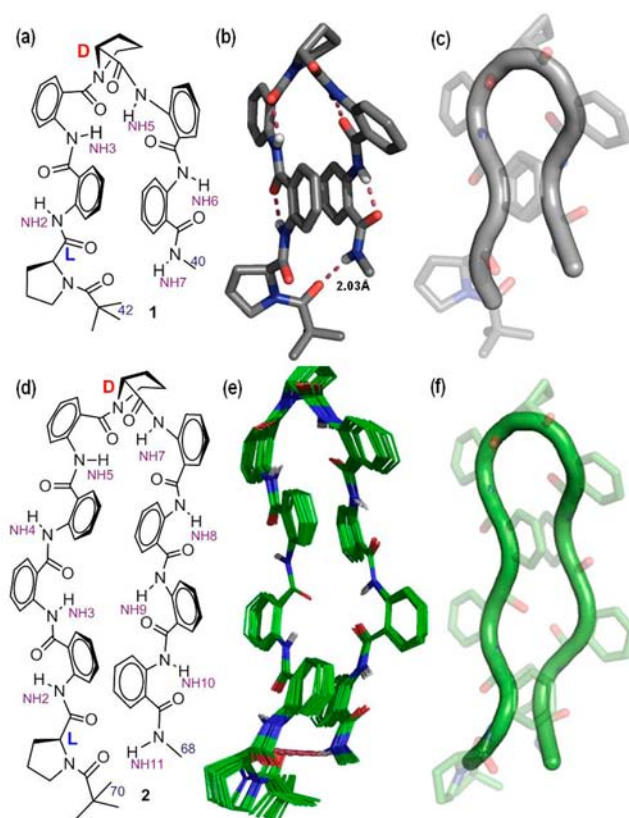


Figure 1. Conformational investigations of zipper peptides **1** and **2**. (a, d) Molecular structure and (c, f) cartoon representation of peptide **1** and its higher analogue **2**, respectively. (b) Crystal structure of **1**. (e) Stereoview of 20 superimposed minimum energy structures of peptide **2** obtained from restrained MD simulations. (Hydrogens, other than the polar amide hydrogens have been removed for clarity).

biopolymers such as leucine zipper regulatory proteins (leucine scissors).¹³

Received: May 31, 2013

Published: July 18, 2013

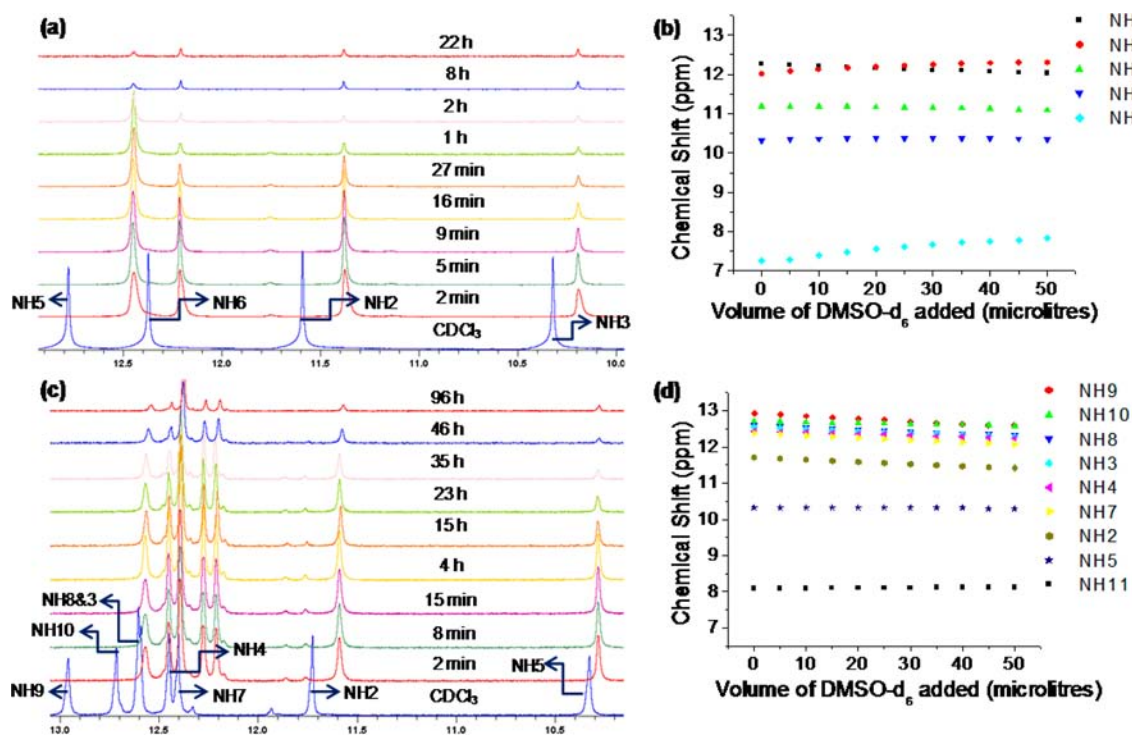


Figure 2. NMR studies of synthetic peptide zippers. ¹H NMR DMSO-*d*₆ titration study (5 mM solution) and ¹H NMR NH/D exchange study in CDCl₃-methanol-*d*₄, respectively of (a,b) hexamer 1 and (c,d) decamer 2. Note: NH₇ of 1 and NH₁₁ of 2 are not displayed in stack plots as they are merged in the aromatic region (full spectra available in SI).

The hetero-chiral hybrid peptides 1 ($n = 2$) and 2 ($n = 4$) of the general sequence ${}^L\alpha\beta_n^D\alpha\beta_n$ feature proline (Pro, a constrained α -amino acid) and anthranilic acid (Ant, a constrained β -amino acid) as building blocks. In order to understand closely the 3D structural architecture of the oligomers, we undertook extensive solid- and solution-state structural studies. Extensive crystallization trials culminated in the formation of crystals of 1.

The striking feature of its crystal structure (Figure 1b) was its unique folded conformation having the oligomer arms zipped together via a long-range intramolecular H-bond, observed at the termini featuring 26 atoms in the H-bonded ring. Aromatic stacking interactions are also clearly evident from the crystal structure. These noncovalent interactions are apparently stronger, characterized by the H-bonding parameters $d(\text{H}\cdots\text{O}) = 2.03 \text{ \AA}$, $d(\text{N}\cdots\text{O}) = 2.848(3) \text{ \AA}$, $(\text{N}-\text{H}\cdots\text{O}) = 153^\circ$, and the torsion angle $(\text{N}-\text{H}\cdots\text{O}=\text{C}) = 8^\circ$, and aromatic proton–aromatic ring centroid distance featuring an edge-to-face stacking effect [$d(\text{C}10 \text{ Ar}-\text{H}-\text{Cg}(5)) = 3.11 \text{ \AA}$ ($\text{Cg} = \text{centroid of Ant5}$)]. Apart from the unusually long-range intramolecular H-bond observed at the termini, all four anthranilic acid residues of 1 display their characteristic six-membered H-bonding interactions usually observed in oligoanthranilamides¹⁴ (Figure 1b).

Conformational investigations of 1 in the solution-state were undertaken using 2D NOESY studies (CDCl₃, 400 MHz). The characteristic long-range inter-residual nOes observed between the groups positioned at the termini ($\text{C}_{42}\text{H}/\text{C}_{40}\text{H}$ and $\text{C}_{42}\text{H}/\text{NH}_7$; SI, Figure S25) were some of the diagnostic dipolar coupling interactions that unambiguously suggested that the solid-state fully folded conformation is clearly prevalent in the solution-state as well. In order to investigate if the larger analogues would assume the similar zipper structure as shown by 1, we synthesized the higher homologue 2, which was

expected to form, if folded the same way as did 1, an H-bonded ring consisting of 46 atoms in the network, in addition to stacking interactions arising out of the zipped conformation. The structural elucidation of 2 was carried out via solution-state NMR studies and MD simulations employing the distance constraints (see the Supporting Information [SI], p S97), as the decapeptide 2 was highly resistant to yield to crystal formation, despite several efforts. Confirmation for the intramolecular nature of H-bondings in 2 was obtained from MeOD exchange studies and DMSO-*d*₆ titration studies (Figure 2d), as described below. Some of the diagnostic dipolar couplings emanating from the terminal interactions in 1 which unequivocally confirmed its folded zipper structure were clearly observed in the case of 2 as well ($\text{C}_{70}\text{H}/\text{C}_{68}\text{H}$ and $\text{C}_{68}\text{H}/\text{NH}_{11}$; see the SI, Figure S27), suggesting similar conformational features.

The peptides 1 and 2 exhibit excellent solubility in nonpolar organic solvents ($\gg 100 \text{ mM}$ in CDCl₃), despite having several amide groups, suggesting the fact that the polar H-bonding groups are not solvent exposed, thereby preventing aggregation. The negligible ¹H NMR chemical shifts ($\Delta\delta \text{ NH}: < 0.15 \text{ ppm}$) observed for the oligomers 1 and 2 up on DMSO-*d*₆ titration studies (up to 10% of DMSO-*d*₆ in CDCl₃) (Figure 2b,d) supported the intramolecular nature of the H-bonds in the solution-state. Further validation for the intramolecular nature of H-bonding was obtained from MeOD exchange studies (Figure 2a,c) where the amide protons could not be completely exchanged even after prolonged time ($> 22 \text{ h}$) (see the SI (SI), Figure S1 and S2).

From the outset, the formation of the terminal long-range inter-residual H-bonding observed in 1 was intriguing, given its large size having 26 atoms in the H-bonded network. Therefore, we were curious to see the outcome if this H-bonding is disengaged. In order to do this, we made the ester analogue 3, lacking an H-bonding amide donor at the C-

terminal, which is essential for H-bonding, as seen in **1**. The difficulty in crystal formation prompted us to investigate its conformation using NOE-based MD simulations employing the distance constraints (see the SI (SI), p S100). The elucidated structure (Figure 3b) reveals substantial fraying at the termini.

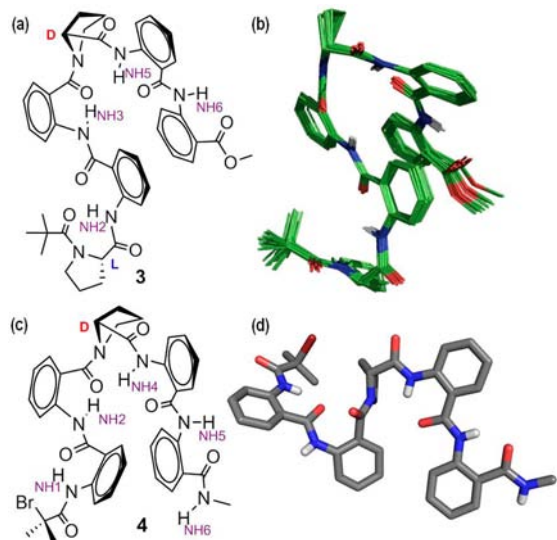


Figure 3. Role of remote H-bonding in the zipper motif formation. (a, c) Molecular structures of hexamer **3** and pentamer **4**, respectively. (b) Stereoview of 20 superimposed minimum energy structures for peptide **3**. (d) Crystal structure of **4**. *Note:* Fraying of the termini in **3** and **4** owing to the lack of terminal H-bonding is evident in the MD structure (b) and crystal structure (d), respectively.

Notably, the diagnostic terminal NOE interactions which were present in **1** were clearly absent in **3**, confirming of fraying of the termini. This result clearly suggests that the long-range inter-residual H-bonding does play a role in maintaining the zipper conformation of the peptide.

In order to further unambiguously confirm the role of terminal H-bonding in the stabilization of the zipper motif, we made the analogue **4** that retains the C-terminal amide NH (as in **1**), but lacks the amide carbonyl acceptor ($-\text{C}=\text{O}$) attached to Pro1 at the N-terminal, which is essential for H-bond ring formation. The presence of bromine in **4**, presumably aided its quick crystallization.^{5f} Investigation of its crystal structure clearly revealed that the termini are driven apart (frayed) owing to the absence of the terminal H-bonding, thus signifying the role of terminal H-bonding in the zipper motif formation (Figure 3d).

The shielding effects observed by aromatic protons can be powerful diagnostic tool to assess the aromatic stacking interactions.⁸ In fact, the first clue to aromatic stacking interactions prevalent in the C-terminal amides **1** and **2** was obtained from their ¹H NMR spectra, wherein the upfield shift experienced by selected aryl protons owing to aromatic stacking interactions was clearly evident (Figure 4a). A closer look at the crystal structure of **1** (Figure 4b) and the NOE-based MD simulated NMR structure of **2** (Figure 4c) further substantiated these *edge-to-face-type*¹⁵ stacking interactions. Distinctive nOes arising from the dipolar coupling between aryl protons (see the SI, Figure S25 and S27) further validated the stacking interactions. It is noteworthy that stacking interactions are poor in the C-terminal ester counterparts of **1** and **2** that show end-fraying, as evident from the absence of comparable upfield

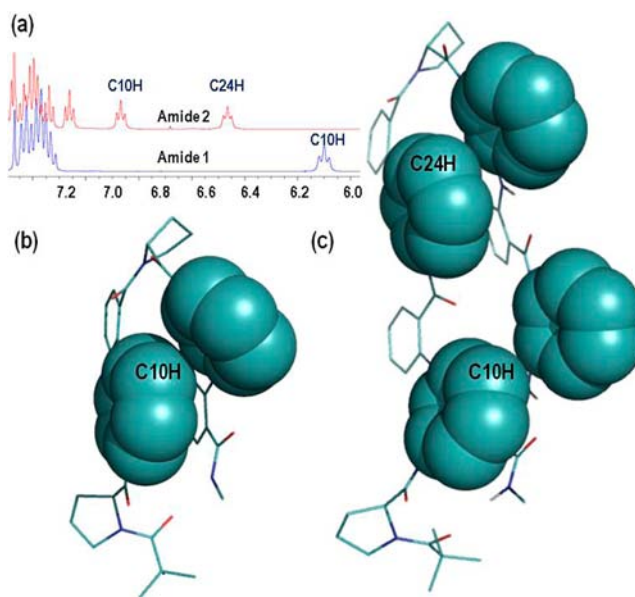


Figure 4. Role of aromatic stacking interactions in the zipper formation. (a) Comparison of the diagnostic ¹H NMR shielding effects observed by amides **1** and **2**. (b) Wireframe representation of crystal structure of amide **1**, (c) MD simulated structure of amide **2**. (*Note:* Aromatic rings bearing upfield protons that observe shielding effects due to aromatic stacking interactions are represented as spheres.)

proton shifts observed in their corresponding amide counterparts **1** and **2**, respectively (see the ¹H spectra in SI, pp S29 and S33).

Having studied the importance of the noncovalent interactions in the zipper motif formation, we studied the effect of chirality on its structural architecture. In order to realize this objective, we made the analogue **5**, which is exactly same as **1**, except that it is homochiral (the second proline is of L chirality). The results confirmed that chirality modulation had a drastic consequence in the zipper architecture, as clearly evident from the crystal structure of **5** (Figure 5). It is noteworthy that alteration of chirality in peptide sequences can have dramatic effect in their overall conformation. A notable case is the high stability of hairpin structures having a ^DPro at the center, when compared to analogous sequences with ^LPro.^{3c} Whereas, the second ^DPro residue in **1** twists the C-terminal arm to come in close proximity with the N-termini, facilitating

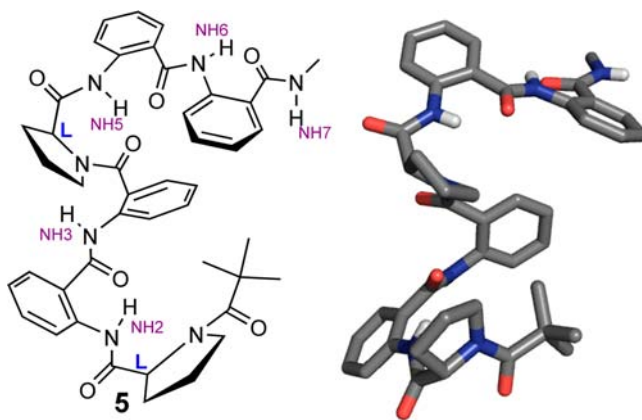


Figure 5. Effect of chirality in folding. Molecular structure (left) and crystal structure (right) of *homo*-chiral hexamer **5**.

the long-range inter-residual H-bonding, the chirality alteration at this region caused dramatic fraying of the termini of **5**, resulting in the C-terminal amide to be exposed to intermolecular H-bonding. Indeed, the intermolecular nature of this amide NH is also clearly supported in the solution-state as judged from solvent titration studies (SI, S53). It is noteworthy that the robust six-membered H-bonding interactions were seen intact in **5** (Figure 5). Thus, our studies on chirality alteration clearly confirm the crucial role played by the Pro residues in maintaining the zipper formation.

In conclusion, this article discloses a unique class of synthetic zipper peptides derived from a blend of α/β -aliphatic/aromatic heterogeneous backbones with different stoichiometric combinations of amino acid residues.¹⁶ These synthetic zipper peptides assume a firm, folded architecture¹⁷ stabilized by complementary aromatic stacking interactions and atypically large remote inter-residual H-bonding interaction.¹⁸ The noncovalent forces that dictate the structural architecture were explored in depth, leading to the conclusion that the zipper structural architecture is governed by a collective cooperative interplay of these noncovalent interactions. Residue selection criteria exert influence over the structural assembly phenomenon, wherein the aromatic stacking forces are anticipated to become more pronounced with larger proportions of aromatic residues, offering more strength to the zipper motif. Structural assembly of the zipper motifs is also greatly controlled by orientational effects of the amino acid residues, signifying the role of the backbone chirality on the conformational bias. The wealth of information accrued from this study suggests that even larger, synthetic zipper peptide analogues can also be envisioned, and efforts are in progress to achieve this objective.

■ ASSOCIATED CONTENT

● Supporting Information

Experimental procedures for compounds **1–5**; ¹H, ¹³C, and DEPT-135 NMR spectra; MALDI-TOF/TOF-mass spectra and 2D spectra of compounds; details of NMR-based MD studies; and crystal data of **1**, **4**, and **5** (CIF). This material is available free of charge via the Internet at <http://pubs.acs.org>.

■ AUTHOR INFORMATION

Corresponding Author

g.j.sanjayan@ncl.res.in (G.J.S.); pr.rajamohan@ncl.res.in (P.R.R.)

Notes

The authors declare no competing financial interests.

■ ACKNOWLEDGMENTS

Dedicated to Prof. K. N. Ganesh and Prof. R. A. Mashelkar on the occasion of their 60th and 70th birthdays, respectively. R.V., S.K., S.R., and A.S.K. thank CSIR, New Delhi, for research fellowships. This work was funded by NCL-IGIB-JRI.

■ REFERENCES

(1) (a) Ayme, J.-F. O.; Beves, J. E.; Leigh, D. A.; McBurney, R. T.; Rissanen, K.; Schultz, D. *Nat. Chem.* **2012**, *4*, 15. (b) Avestro, A.-J.; Belowich, M. E.; Stoddart, J. F. *Chem. Soc. Rev.* **2012**, *41*, 5881. (c) Ruangsapichat, N.; Pollard, M. M.; Harutyunyan, S. R.; Feringa, B. L. *Nat. Chem.* **2011**, *3*, 53. (d) Hasell, T.; Wu, X.; A., J. T.; Bacsa, J.; Steiner, A.; Mitra, T.; Trewin, A.; Adams, D. J.; Cooper, A. I. *Nat. Chem.* **2010**, *2*, 750.

(2) (a) Smulders, M. M. J.; Riddell, I. A.; Browne, C.; Nitschke, J. R. *Chem. Soc. Rev.* **2013**, *42*, 1728. (b) Aida, T.; Meijer, E. W.; Stupp, S. I. *Science* **2012**, *335*, 813. (c) Ousaka, N.; Takeyama, Y.; Iida, H.; Yashima, E. *Nat. Chem.* **2011**, *3*, 856. (d) Wang, Q.; Mynar, J. L.; Yoshida, M.; Lee, E.; Lee, M.; Okuro, K.; Kinbara, K.; Aida, T. *Nature* **2010**, *463*, 339.

(3) (a) Horne, W. S.; Gellman, S. H. *Acc. Chem. Res.* **2008**, *41*, 1399. (b) Seebach, D.; Gardiner, J. *Acc. Chem. Res.* **2008**, *41*, 1366. (c) Vasudev, P. G.; Chatterjee, S.; Shamala, N.; Balaram, P. *Chem. Rev.* **2011**, *111*, 657. (d) Martinek, T. A.; Fulop, F. *Chem. Soc. Rev.* **2012**, *41*, 687. (e) Pilsl, L. K. A.; Reiser, O. *Amino Acids* **2011**, *41*, 709. (f) Tomasini, C.; Angelici, G.; Castellucci, N. *Eur. J. Org. Chem.* **2011**, *2011*, 3648. (g) Roy, A.; Prabhakaran, P.; Baruah, P. K.; Sanjayan, G. J. *Chem. Commun.* **2011**, *47*, 11593.

(4) (a) Porter, E. A.; Wang, X. H.; Lee, S.; Weisblum, B.; Gellman, S. H. *Nature* **2000**, *404*, 565. (b) Cheng, P.-N.; Liu, C.; Zhao, M.; Eisenberg, D.; Nowick, J. S. *Nat. Chem.* **2012**, *4*, 927. (c) Scheck, R. A.; Schepartz, A. *Acc. Chem. Res.* **2011**, *44*, 654. (d) Goodman, C. M.; Choi, S.; Shandler, S.; DeGrado, W. F. *Nat. Chem. Biol.* **2007**, *3*, 252.

(5) (a) Johnson, L. M.; Mortenson, D. E.; Yun, H. G.; Horne, W. S.; Ketas, T. J.; Lu, M.; Moore, J. P.; Gellman, S. H. *J. Am. Chem. Soc.* **2012**, *134*, 7317. (b) Berlicki, L.; Pilsl, L.; Weber, E.; Mándity, I. M.; Cabrele, C.; Martinek, T. A.; Fülöp, F.; Reiser, O. *Angew. Chem., Int. Ed.* **2012**, *51*, 2208. (c) Prabhakaran, P.; Kale, S. S.; Puranik, V. G.; Rajamohan, P. R.; Chetina, O.; Howard, J. A. K.; Hofmann, H.-J.; Sanjayan, G. J. *J. Am. Chem. Soc.* **2008**, *130*, 17743. (d) Vijayadas, K. N.; Davis, H. C.; Kotmale, A. S.; Gawade, R. L.; Puranik, V. G.; Rajamohan, P. R.; Sanjayan, G. J. *Chem. Commun.* **2012**, *48*, 9747. (e) Priya, G.; Kotmale, A. S.; Gawade, R. L.; Mishra, D.; Pal, S.; Puranik, V. G.; Rajamohan, P. R.; Sanjayan, G. J. *Chem. Commun.* **2012**, *48*, 8922. (f) Thorat, V. H.; Ingole, T. S.; Vijayadas, K. N.; Nair, R. V.; Kale, S. S.; Ramesh, V. V. E.; Davis, H. C.; Prabhakaran, P.; Gonnade, R. G.; Gawade, R. L.; Puranik, V. G.; Rajamohan, P. R.; Sanjayan, G. J. *Eur. J. Org. Chem.* **2013**, 3529 and refs cited therein.

(6) Ramachandran, G. N.; Kartha, G. *Nature* **1955**, *176*, 593.

(7) (a) Gong, B. *Acc. Chem. Res.* **2012**, *45*, 2077. (b) Hunter, C. A.; Spitaleri, A.; Tomas, S. *Chem. Commun.* **2005**, 3691. (c) Brüggemann, J.; Bitter, S.; Müller, S.; Müller, W. M.; Müller, U.; Maier, N. M.; Lindner, W.; Vögtle, F. *Angew. Chem., Int. Ed.* **2007**, *46*, 254.

(8) (a) Klarner, F.-G.; Schrader, T. *Acc. Chem. Res.* **2012**, *46*, 967. (b) Salonen, L. M.; Ellermann, M.; Diederich, F. *Angew. Chem., Int. Ed.* **2011**, *50*, 4808.

(9) Kool, E. T. *Chem. Rev.* **1997**, *97*, 1473–1488.

(10) Delaurière, L.; Dong, Z.; Laxmi-Reddy, K.; Godde, F.; Toulmé, J.-J.; Huc, I. *Angew. Chem., Int. Ed.* **2012**, *51*, 473.

(11) (a) Gan, Q.; Ferrand, Y.; Bao, C.; Kauffmann, B.; Grélard, A.; Jiang, H.; Huc, I. *Science* **2011**, *331*, 1172. (b) Prabhakaran, P.; Priya, G.; Sanjayan, G. J. *Angew. Chem., Int. Ed.* **2012**, *51*, 4006.

(12) Nelson, J. C.; Saven, J. G.; Moore, J. S.; Wolynes, P. G. *Science* **1997**, *277*, 1793.

(13) Krylov, D.; Vinson, C. R. Leucine Zipper. In *eLS [Encyclopedia of Life Sciences]*; John Wiley & Sons, Ltd.: New York, 2001.

(14) (a) Hamuro, Y.; Geib, S. J.; Hamilton, A. D. *J. Am. Chem. Soc.* **1997**, *119*, 10587. (b) Hamuro, Y.; Geib, S. J.; Hamilton, A. D. *J. Am. Chem. Soc.* **1996**, *118*, 7529.

(15) Tatko, C. D.; Waters, M. L. *J. Am. Chem. Soc.* **2002**, *124*, 9372.

(16) The zipper architecture observed herein is markedly different from the right-handed helical architecture formed of Ant and Pro residues in 1:1 ratio (see ref 5c).

(17) Crystallographic data of **1**, **4**, and **5** have been deposited with the Cambridge Crystallographic Data Centre: CCDC: 913431, 913432, and 913433 for **1**, **4**, and **5**, respectively.

(18) For related systems featuring zipper architectures, see: (a) Archer, E. A.; Krische, M. J. *J. Am. Chem. Soc.* **2002**, *124*, 5074. (b) Zhao, X.; Jia, M.-X.; Jiang, X.-K.; Wu, L.-Z.; Li, Z.-T.; Chen, G.-J. *J. Org. Chem.* **2003**, *69*, 270 and refs 4b and 7a.